ISSN 2720-3581

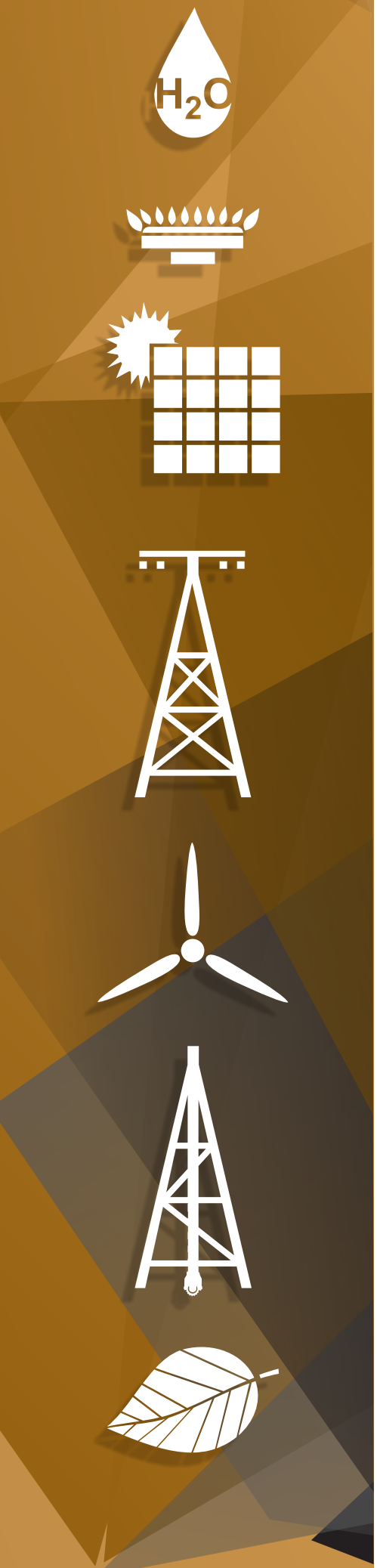

JOURNAL OF GEOTECHNOLOGY AND ENERGY

FORMERLY AGH DRILLING, OIL, GAS

2023, vol. 40, no. 4

WYDAWNICTWA AGH

KRAKOW 2023

ISSN 2720-3581

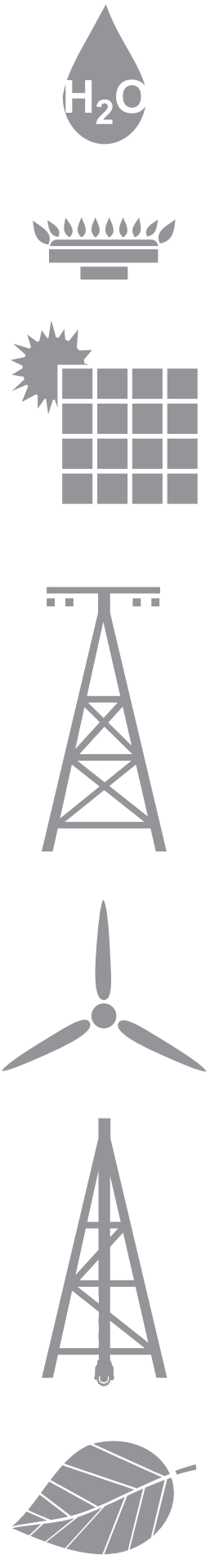

JOURNAL OF GEOTECHNOLOGY AND ENERGY

FORMERLY AGH DRILLING, OIL, GAS

2023, vol. 40, no. 4

WYDAWNICTWA AGH

KRAKOW 2023

The "Journal of Geotechnology and Energy" (formerly "AGH Drilling, Oil, Gas") is a quarterly published by the Faculty of Drilling, Oil and Gas at the AGH University of Krakow, Poland. Journal is an interdisciplinary, international, peer-reviewed, and open access. The articles published in JGE have been given a favorable opinion by the reviewers designated by the editorial board.

Editorial Team

Publisher

AGH University Press

Linguistic corrector: *Aeddan Shaw*
Technical editor: *Kamila Zimnicka*
Desktop publishing: *Munda*
Cover design: *Paweł Sepielak*

ISSN: 2720-3581
DOI: https://doi.org/10.7494/jge

Journal website: https://journals.agh.edu.pl/jge

Wydawnictwa AGH (AGH University Press)
al. A. Mickiewicza 30, 30-059 Kraków
tel. 12 617 32 28, 12 636 40 38
e-mail: redakcja@wydawnictwoagh.pl
www.wydawnictwo.agh.edu.pl

CONTENTS

Journal of Geotechnology and Energy | vol. 40 | no. 4 | 2023 | pp. 5–14

https://doi.org/10.7494/jge.2023.40.4.5918

ARTICLE

Aneta Sapińska-Śliwa

AGH University of Krakow, Laboratory of Geoenergetics
ORCID: 0000-0002-2728-3413

Remigiusz Kunasz

AGH University of Krakow, Laboratory of Geoenergetics
ORCID: 0009-0000-3875-0630

Tomasz Śliwa

AGH University of Krakow, Laboratory of Geoenergetics
ORCID: 0000-0002-7005-8190
e-mail: sliwa@agh.edu.pl

ANALYSIS OF THE POTENTIAL HEATING OF SELECTED STUDENT RESIDENCES AT THE AGH UNIVERSITY OF KRAKOW USING THE EARTH'S HEAT

Date of submission:
24.11.2023

Date of acceptance:
26.12.2023

Date of publication:
29.12.2023

https://journals.agh.edu.pl/jge

Abstract: The aim of this study was to adapt the operating parameters of a geothermal heat pump system to the required average power needed to meet the energy for central heating and domestic hot water of selected student residences. Calculations of the average power required by the dormitories in the AGH University Student Campus were carried out, as well as modelling of the deep borehole heat exchanger for the heating load. The designed heating system for the student residences in the AGH University Student Campus using a deep borehole heat exchanger – is sufficient to cover the base heat demand for five four-storey dormitories. During the writing of the paper, the main problem was the low availability of articles on deep borehole heat exchangers. This is due to the continuous development and testing of new engineering ideas.

Deep borehole heat exchangers can be use as new boreholes or wells prepared for liquidation. Also use of closed boreholes sometimes is possible, depending on project of liquidation. The future districy heating will use low-temperature heat carrier for heating and cooling. Use borehole fields as rockmass use for heat and/or cool ,storage will be common.

Keywords: deep borehole heat exchanger, geoenergetics, geothermal, drilling

1. Introduction

Annually increasing global energy prices have fuelled the public's interest in geothermal energy, accelerating the development of efficient ways of extracting heat energy from the rock mass.

The aim of this study is to show that the Earth's heat is suitable for the efficient heating of student residences at the AGH University of Krakow. There are many possible options, including a deep borehole heat exchanger.

Geothermal is a branch of economy and science encompassing the exploration, access, exploitation (extraction and injection), transport, processing and use of geothermal energy (whose source is the planet Earth) or the Earth's heat (contained in rock mass, solar and anthropogenic) [1].

Geothermal energy, extracted from rocks and groundwater, is most generally characterised by a division into two types: high-temperature, medium-temperature and low-temperature. High-temperature geothermal offers the possibility of using the Earth's heat to generate electricity. The means of heat transfer are high-temperature fluids that fill the pore space of the permeable layer. Medium-temperature thermal waters are used for direct heating in heating systems and for power generation in binary power plants [2]. Sources of geothermal energy that have temperatures low enough to recover thermal energy without the use of heat pumps are knowna as low-temperature geothermal [3].

The most effective method of making heat available is thermal water exploitation, where the heat carrier (water) is brought to the surface through an exploitation borehole that delivers the fluid through extraction pipes or a full section. This is a single-hole operation discharging the used water into surface watercourses. A system that includes a single borehole is only used when aquifer recharge conditions are very good. When geological conditions do not allow the rapid regeneration of water resources, a single-hole exploitation and absorption system is used. The cooled water is injected through an annular space into the absorption layer and the fluid is extracted from the geothermal layer through extraction pipes. Another method is the two-well extraction-absorption system (geothermal doublet), which involves injecting a reduced-temperature heat carrier into the geothermal layer via an absorption well. The extraction of high-temperature geothermal water is carried out through an exploitation well [2].

The Hot Dry Rock (HDR) heat extraction system involves extracting heat from dry volcanic, deep-sea and metamorphic rocks. Deposits of such rocks are found at depths of 3–6 km (excluding volcanic zones). The exploitation of this system is based on the circulation of water forced by pumps in a permeable geological reservoir or one where an artificial fracture zone has been created. Water is transported through a borehole to the fractured high-temperature rocks. A second borehole brings hot steam to the surface [2].

Borehole heat exchangers are an installation that allows heat to be transported from or to the rock mass. They are used in many countries around the world on an ever-increasing scale for heating and cooling systems that operate in conjunction with heat pumps. The system, in which either water or a glycol solution circulates, is closed. There are different types of design (Figs. 1–5):

– single U-tube,

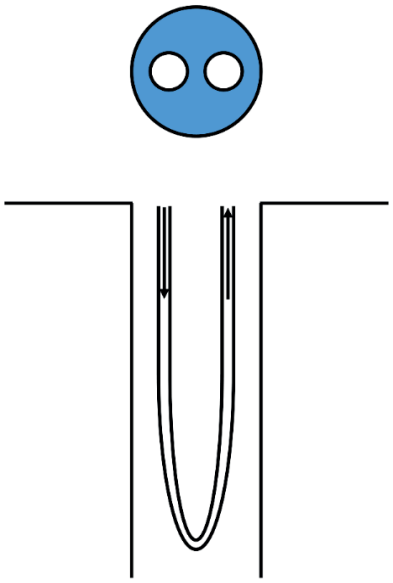

Fig. 1. Single U-tube

– double U-tube,

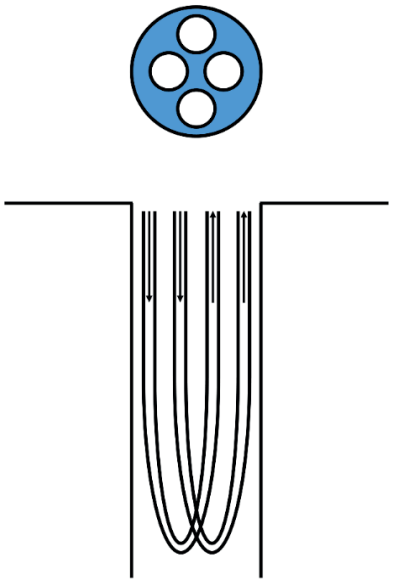

Fig. 2. Double U-tube

– coaxial system,

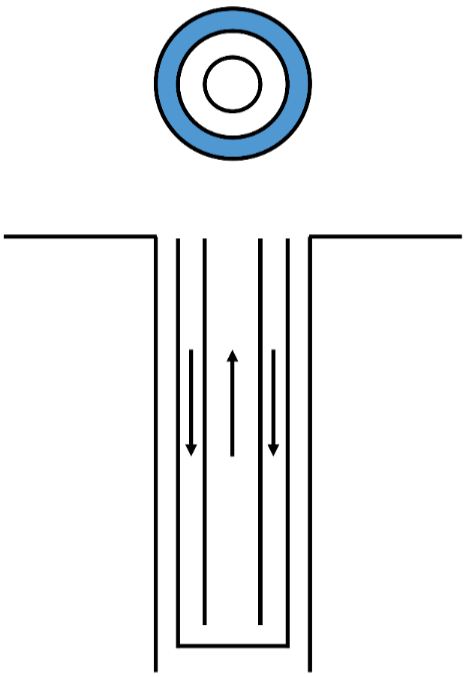

Fig. 3. Coaxial system

– 3-tube system (1 × larger diameter, 2 × smaller diameter),

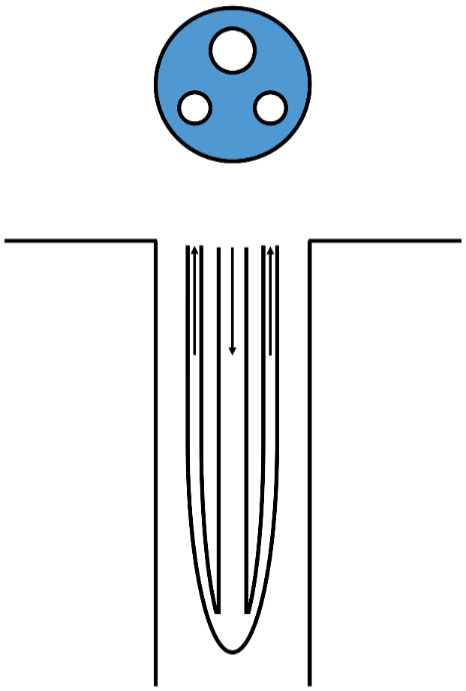

Fig. 4. 3-tube system (1 × larger diameter, 2 × smaller diameter)

– 3-tube system (3 × identical diameter),

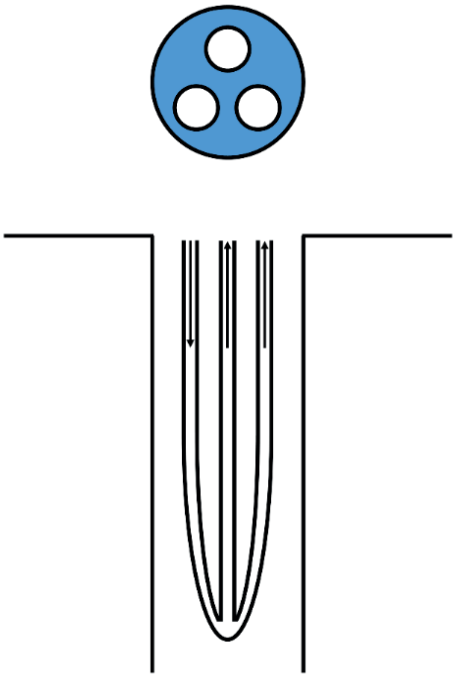

Fig. 5. 3-tube system (3 × identical diameter)

The U-tube material is polyethylene (PE) due to its high thermal conductivity coefficient. The centric system consists of two tubes: an outer tube (a material with a high thermal conductivity coefficient) and an inner tube (a material with a low thermal conductivity coefficient). U-tubes are typically used up to a depth of 150 m, deeper than that at which a centric design is used [4]. The drilling depth of a borehole heat exchanger is related to both geological conditions and cost. Closely related to the geology is the drilling method employed. When drilling in rocks of lower hardness, the rotary mud method is used. On the other hand, when drilling through harder strata, the percussion rotary method is a much more efficient and easier drilling method. Unfortunately, it is significantly more expensive [5]. Borehole heat exchangers have a number of advantages, which include the following [6]:

– minimal environmental impact,
– the possibility of operating as a heat and cooling source,
– very good long-term reliability of the system,
– significant energy savings during cooling compared with traditional methods.

There is a lot of global interest in borehole heat exchangers today. The vast majority of these are shallow boreholes with depths of tens to hundreds of metres. The use of deep boreholes (2 000–4 000 m) for the installation

of deep borehole heat exchangers (DBHE) makes it possible to obtain higher working fluid temperatures and more energy [7]. In contrast to shallow installations, a deep borehole heat exchanger is only able to convert energy for heating purposes. Due to the high rock temperatures in the rock mass, it is impossible to use such exchangers for cooling purposes. Given the high costs of drilling boreholes, existing boreholes that were drilled for other purposes, such as negative exploration boreholes or depleted oil wells, are usually considered for investment [4].

2. Methodology

Average power (P):

$$P = \frac{Q}{t} \tag{1}$$

where:
Q – heat supplied (thermal energy consumption) [J],
t – time at which the heat was delivered [s].

Calculations of the effective thermal parameters of the rocks along with the average temperature in the borehole have been made below.

Weighted average thermal conductivity of the rocks:

$$\lambda_{av} = \frac{\lambda_1 \cdot h_1 + \lambda_2 \cdot h_2 + \ldots + \lambda_i \cdot h_i}{h_1 + h_2 + \ldots + h_i} \left[\frac{\mathrm{W}}{\mathrm{m \cdot K}}\right] \tag{2}$$

where:
λ_i – thermal conductivity of a given rock layer [W· m^{-1}·K^{-1}],
h_i – thickness of given rock layer [m].

Weighted average of rock heat capacity:

$$c_{v_{av}} = \frac{c_{v1} \cdot h_1 + c_{v2} \cdot h_2 + \ldots + c_{vi} \cdot h_i}{h_1 + h_2 + \ldots + h_i} \left[\frac{\mathrm{MJ}}{\mathrm{m^3 \cdot K}}\right] \tag{3}$$

where:
c_{vi} – heat capacity of a given rock layer [MJ·m^{-3}·K^{-1}],
h_i – thickness of given rock layer [m].

Average temperature in the borehole:

$$T_{av} = \frac{T_0 + T_{3\,000\,\mathrm{m}}}{2} \ [^\circ\mathrm{C}] \tag{4}$$

$$T_{3\,000\,\mathrm{m}} = T_0 + G \cdot (H - h_i) \ [^\circ\mathrm{C}] \tag{5}$$

where:
T_0 – average annual temperature at ground level in Krakow – 8.6°C,
G – geothermal gradient – 3°C/100 m,
H – depth of borehole – 3 000 m,
h_0 – depth of periodic heat penetration – 15 m.

For mathematical modelling and operational forecasting, data is still needed on:
- The coaxial exchanger pipe system will be installed in a vertical borehole with a depth 3 000 m.
- The weighted average (after thickness) thermal conductivity of the rock is, $\lambda = 2.621$ W·m^{-1}·K^{-1}.
- The weighted average (after thickness) volumetric heat capacity is, $c_v = 2.312$ MJ·m^{-3}·K^{-1}.
- The average temperature in the borehole is, $T = 53.375$°C.
- Heat carrier parameters:
  - water at a temperature, $T = 10$°C, as the heat carrier in the system,
  - thermal conductivity: 0.582 W·m^{-1}·K^{-1},
  - specific heat: 4 192 J·kg^{-1}·K^{-1},
  - density: 999.8 kg·m^{-3},
  - viscosity: 0.001308 kg·m^{-1}·s^{-1},
  - freezing point: 0°C.
- Inner pipe parameters:
  - outer diameter: 114.3 mm,
  - wall thickness: 12.7 mm,
  - thermal conductivity: 0.02 W·m^{-1}·K^{-1}.
- Outer pipe parameters:
  - outer diameter: 177.8 mm,
  - wall thickness: 11.51 mm,
  - thermal conductivity: 50 W·m^{-1}·K^{-1}.
- Heat carrier flow rate, $Q = 3.33$ dm^3·s^{-1}.
- Thermal conductivity of the sealing slurry, $\lambda = 1.2$ W·m^{-1}·K^{-1}.
- Thermal conductivity of vacuum insulated tubing (VIT), $\lambda = 0.02$ W·m^{-1}·K^{-1}.
- Heat pump coefficient of performance, COP = 4.
- Base load (central heating + domestic hot water) monthly for one four-storey student house, as an average of student houses 15, 16 and 17 in 2017 due to the highest consumption from 2016 to 2020.

Mathematical model is based on the commercial softwear Earth Energy Designer (EEE ver. 4.1). In cylindrical coordinates, the ground temperature fulfills the heat conduction equation:

$$\frac{1}{\alpha}\frac{\partial T}{\partial t} = \frac{\partial^2 T}{\partial r^2} + \frac{1}{r}\frac{\partial T}{\partial r} + \frac{\partial^2 T}{\partial x^2}$$

Both the beginning state under the ground and the boundary condition at the Earth's surface are:

$$T(r,0,t) = T_{ON}$$

$$T(r,x,0) = T_{ON}$$

Particular consideration must be given to the boundary conditions at the borehole wall. Throughout the borehole's length, the temperature remains constant:

$$T(r_b, z, t) = T_b(t)$$

$$D < x < D + H$$

The heat extraction rate $q(t)$ is given by:

$$q(t) = \frac{1}{H} \int_{D}^{D+H} 2\pi r \lambda \frac{\partial T}{\partial r}$$

For the entire boundary condition, $T_b(t)$ or $q(t)$ might be prescribed.

Softwear works with use methodology of g-function, as quasi numerical solution of multi well field. For described example it is not used. The analysis covers one borehole heat extraction/injection. So the module of g-function is not necessary. EED4.1 based on multipoles method – a method from the group of superposition methods

The softear/model has limitations, the most important being the groundwater flow rate in watered layers. This can be improved by making long-time thermal response tests [8].

3. Calculation

The necessary calculations for the power required by the student part of the AGH University Student Campus residences and the thermal parameters of the rocks present in the lithological section at the project site are included below.

3.1. Calculation of the average power required by the AGH University Student Campus residences

On the basis of the data on thermal energy consumption (central heating and domestic hot water) from 2016 to 2020 made available by the AGH University Student Campus management, the average power required by the student residences was calculated.

Example: January 2017 – DS 7 (central heating + domestic hot water).

$P = (364 \cdot 10^9 \text{ J})/(2678400 \text{ s}) = 135\,902.031 \text{ W}$
$= 135.902 \text{ kW}$

The colours, from dark red to dark green, indicate the increasing average power (Tab. 1) and heat consumption (Tab. 2) of the individual student residence in a given year.

Table 1. Average power required by AGH student residences in 2016–2020 (source: own analysis based on AGH University data), DS and ALFA DS – students dormitories

Student dormitory	Average power [kW]				
	2016	2017	2018	2019	2020
DS 1 "Olimp"	172.220	145.548	126.427	137.620	104.148
DS 2 "Babilon"	157.072	148.592	141.299	148.846	113.685
DS 3 "Akropol"	149.672	181.443	169.267	158.644	130.857
DS 4	27.575	39.859	61.739	67.764	49.870
DS 5	47.055	48.104	44.394	45.408	39.845
DS 6	58.629	60.312	53.526	57.236	43.355
DS 7	62.898	71.759	65.576	57.204	51.577
DS 8	60.021	73.503	68.715	57.585	48.194
DS 9	61.412	62.310	57.046	58.219	47.877
DS 10	59.546	56.380	50.736	49.784	25.330
DS 11	59.957	57.236	54.509	52.765	29.157
DS 12	62.139	62.627	18.899	44.203	35.576
DS 13	63.816	65.290	64.498	43.791	14.325
DS 14 "Kapitol"	184.142	174.689	172.913	167.523	139.490
DS 15	63.816	67.352	41.254	27.841	38.485
DS 16	66.187	65.703	62.722	61.866	54.107
DS 17	51.799	55.778	49.721	48.706	39.213
DS 18	70.994	25.051	63.356	62.690	63.879
DS 19	49.395	54.192	49.689	53.050	47.877
"Alfa"	233.505	265.791	274.575	289.384	230.912
Total	1 761.852	1 781.520	1 690.861	1 690.132	1 347.760

The Table 2 shows the heat consumption of student residences 15, 16 and 17 from 2016 to 2020, the analysed buildings are underlined.

Figure 6 provides a summary of the average annual power consumed by all student residences at the AGH University Student Campus between 2016 and 2020.

Table 2. Thermal energy consumption in GJ (central heating + domestic hot water) in student residences 15, 16, 17 in 2016–2020 (source: data of AGH University of Krakow)

Month	2016			2017			2018			2019			2020		
	Student residence number														
	15	16	17	15	16	17	15	16	17	15	16	17	15	16	17
January	360	331	275	360	348	306	338	315	266	0	395	327	185	259	211
Febuary	243	234	202	278	271	248	355	334	277	0	229	184	227	214	161
March	284	277	223	256	248	199	296	291	249	0	211	168	101	215	187
April	176	183	135	203	198	145	121	155	111	121	202	146	114	158	99
May	110	181	101	145	161	120	76	114	85	96	137	99	71	48	50
June	75	84	65	71	95	68	55	77	58	68	73	51	38	55	40
July	24	36	34	34	34	43	55	46	34	75	38	38	29	50	23
August	27	32	35	39	31	41	5	22	16	49	60	30	21	52	0
Septempber	22	32	17	45	42	50	0	37	19	32	44	27	32	62	11
October	159	179	123	164	166	125	0	183	119	124	80	102	112	210	123
November	243	245	195	296	266	230	0	219	178	132	196	136	132	175	148
December	295	279	233	233	212	184	0	185	156	181	286	228	155	213	187

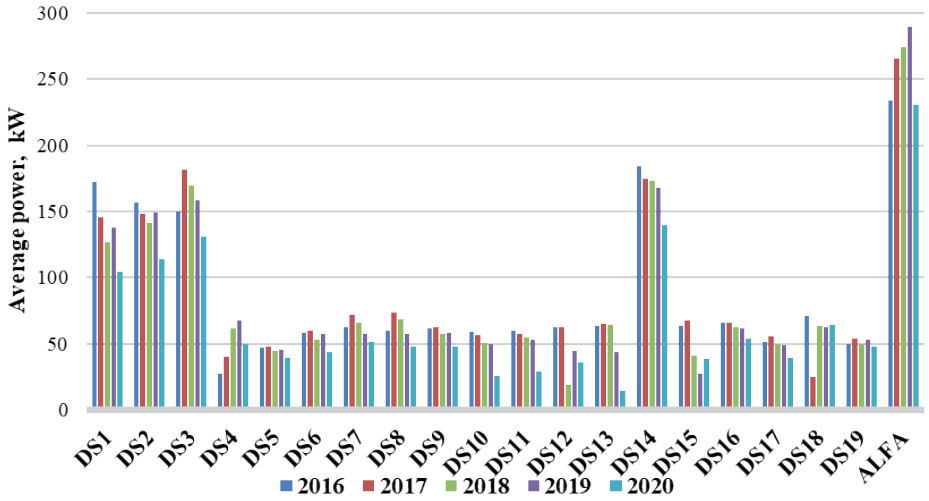

Fig. 6. Average annual power consumed in AGH student campus residences between 2016 and 2020, DS and ALFA – students dormitories

3.2. Calculation of rock thermal parameters and average temperature in the borehole

Table 3 shows the different layers present in the rock mass along with their thickness and thermal parameters.

$$\lambda_{av} = 2.621 \ \frac{\mathrm{W}}{\mathrm{m \cdot K}}$$

$$c_{v_{av}} = 2.312 \ \frac{\mathrm{MJ}}{\mathrm{m^3 \cdot K}}$$

$$T_{3\,000\,\mathrm{m}} = 98.15^{\circ}\mathrm{C}$$

$$T_{av} = 53.375^{\circ}\mathrm{C}$$

Table 3. Lithological profile of the strata with thermal parameters

Layer	Depth of layer [m]		Thermal conductivity λ [W·m^{-1}·K^{-1}]	Specific heat capacity c_v [MJ·m^{-3}·K^{-1}]
Siltstones, shales	0	172	2.20	2.27
Grey zailone sandstones	172	327	2.16	2.00
Diabase	327	423	2.80	2.22
Fine-grained grey sandstones	423	498	2.22	2.09
Shales, siltstones	498	764	2.20	2.27
Fine-grained sandstones zailone	764	929	2.30	1.70
Dark grey shales, dark grey siltstones	929	1 160	2.20	2.22
Grey and dark grey limestones	1 160	1 452	2.80	2.35
Dolomitic limestones, dolomites 30/70	1 452	1 684	2.55	2.30
Beige and grey-beige dolomites	1 684	1 888	3.20	2.50
Grey and dark grey limestones, dolomitic limestones 10/90	1 888	2 349	2.38	2.41
Beige and grey-beige dolomites	2 349	3 000	3.20	2.50

3.3. Assumptions for the DBHE project

Below are the assumptions, i.e. the parameters with the values that were used to simulate the operation of the exchanger for up to 25 years of operation.

- The coaxial exchanger pipe system will be installed in a vertical borehole with a depth, H = 3 000 m.
- The weighted average (after thickness) thermal conductivity of the rock is, λ = 2.621 W·m^{-1}·K^{-1}.
- The weighted average (after thickness) volumetric heat capacity is, c_v = 2.312 MJ·m^{-3}·K^{-1}.
- The average temperature in the borehole is, T = 53.375°C.
- Heat carrier parameters:
  - water at a temperature, T = 10°C, as the heat carrier in the system,
  - thermal conductivity: 0.582 W·m^{-1}·K^{-1},
  - specific heat: 4192 J·kg^{-1}·K^{-1},
  - density: 999.8 kg·m^{-3} ,
  - viscosity: 0.001308 kg·m^{-1}·s^{-1},
  - freezing point: 0°C.
- Inner pipe parameters:
  - outer diameter: 114.3 mm,
  - wall thickness: 12.7 mm,
  - thermal conductivity: 0.02 W·m^{-1}·K^{-1}.
- Outer pipe parameters:
  - outer diameter: 177.8 mm,
  - wall thickness: 11.51 mm,
  - thermal conductivity: 50 W·m^{-1}·K^{-1}.
- Heat carrier flow rate, Q = 3.33 dm^3·s^{-1}.
- Thermal conductivity of the sealing slurry, λ = 1.2 W·m^{-1}·K^{-1}.
- Thermal conductivity of vacuum insulated tubing (VIT), λ = 0.02 W·m^{-1}·K^{-1}.
- Heat pump coefficient of performance, COP = 4.
- Base load (central heating + domestic hot water) monthly for one four-storey student house, as an average of student houses 15, 16 and 17 in 2017 due to the highest consumption from 2016 to 2020.

3.4. Simulation of deep borehole heat exchanger operation

Simulations for the loading of the deep borehole heat exchanger were carried out in the "Earth Energy Designer" (EED) software for different variants:

- one four-storey student house,
- three four-storey student residences,
- five four-storey student residences,
- six four-storey student residences.

For the simulation of deep heat exchangers in the EED programme, the temperature at the ground surface is equal to the average temperature in the borehole.

The load for one student house is shown in Figure 7, Figure 8 shows the load for three student houses, Figure 9 shows the load for five student houses and Figure 10 shows the load for six student houses.

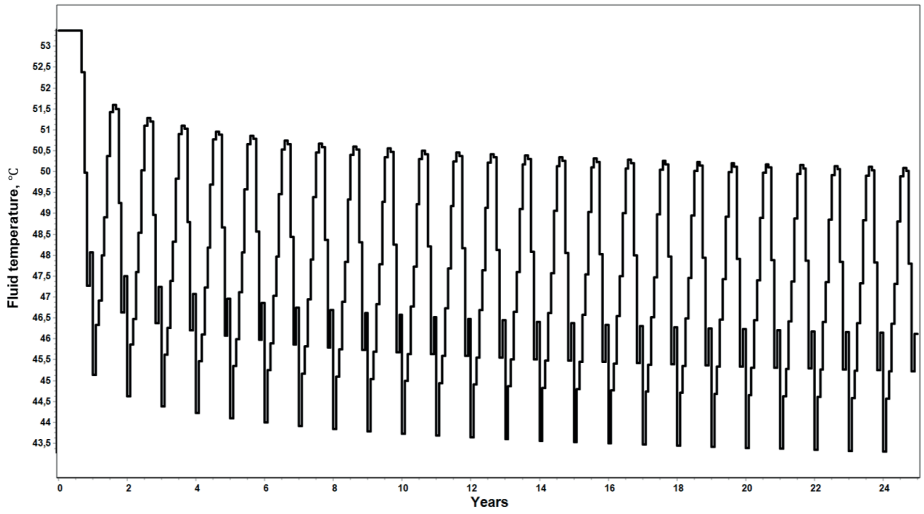

Fig. 7. Heat carrier temperature as a function of simulation time for one four-storey dormitory

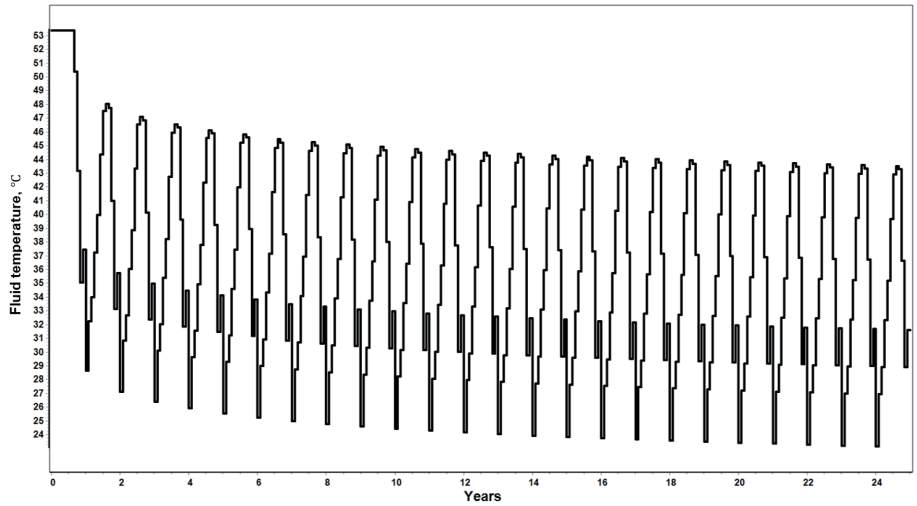

Fig. 8. Heat carrier temperature depending on simulation time for three four-storey dormitories

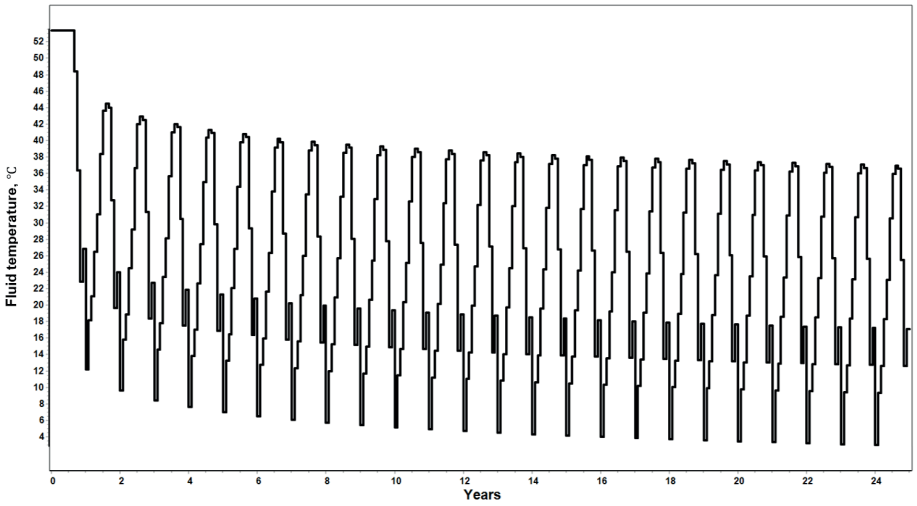

Fig. 9. Heat carrier temperature depending on simulation time for five four-storey dormitories

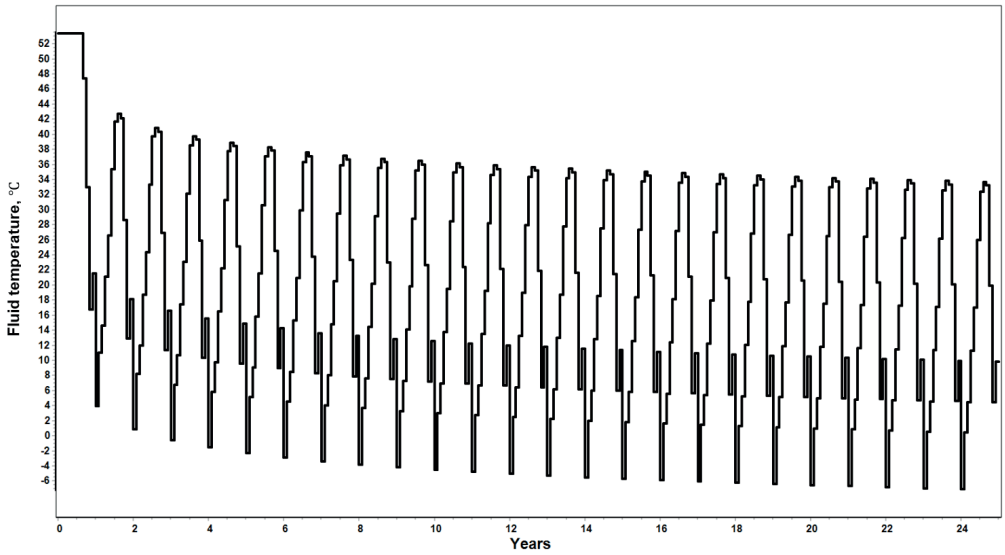

Fig. 10. Heat carrier temperature as a function of simulation time for six four-storey dormitories

4. Conclusions

1. The Alpha, Acropolis, Babylon, and Olympus student residences consume the most heat energy per year. This is shown in Figure 6 as heating power.
2. All four-storey student residences in the AGH University Student Campus consume a similar amount of heat energy per year, which covers interior (central) heating and domestic warm water.
3. The deep borehole heat exchanger cooperating with the geothermal heat pump will allow for the heating energy needs of the five four-storey dormitories in the AGH University Student Campus to be satisifed. A single dormitory can be heated without heat pump.
4. It may be possible to heat single four-storey student house without a heat pump due to the high temperature of the heat carrier of over 43°C in year 25 of the simulation, during the peak heating load. When the temperature of heating system after thermomodernization drops, more dormitories could work without heat pumps. Another solution is domestic warm water heating for more dormitories, but the data of heat demand were not separated for d.w.w and central heating.
5. Six student residences cannot be heated due to the temperature of the heat carrier dropping below the freezing point. Already in the third year of operation, a reduction in the average temperature of the heat carrier in the borehole heat exchanger below 0°C can be observed (Fig. 10). In such a system, heat exploitation is possible, but with the use of an aqueous solution of glycole as heat carrier. The low thermal conductivity of the heat exchanger inner pipe is very important for isolating the inflowing heat carrier from the outflowing heat carrier, especially at low depths near the ground surface. Because of the model limitations, the energy output of DBHE may be higher if the flow of underground water is present.
6. In the near future, the authors suggest working on the mathematical method with groundwater flow. However, this is limited by the need for geological data before drilling.

The replacement of traditional energy sources in district heating networks by geothermal sources should be carried out in conjunction with the thermal modernisation of buildings. As part of this thermomodernisation, attention should not only be paid to changes in power and heat demand, but also to the parameters of the heating system. Any reduction in the heating system supply temperature will facilitate an increase in the load on geothermal sources, including geothermal heat pumps.

Acknowledgements: The work was created under the subsidy of the Department of Drilling and Geoengineering No. 16.16.190.779 (Faculty of Drilling, Oil and Gas AGH University of Krakow).

References

[1] Śliwa T.: *Grawitacyjne otworowe magazyny energii – potencjał na przykładzie złoża Przemyśl*. 13. Polski Kongres Naftowców i Gazowników, Bóbrka, 2–3 czerwca 2022, https://www.sitpnig.pl/single-post/13-polski-kongres-naftowc%C3%B3w-i-gazownik%C3%B3w-b%C3%B3brka-2-3-czerwca-2022-r

[2] Gonet A. (red.): *Metodyka identyfikacji potencjału cieplnego górotworu wraz z technologią wykonywania i eksploatacji otworowych wymienników ciepła*. Wydawnictwa AGH, Kraków 2011.

[3] Ryżyński G., Majer E.: *Geotermia niskotemperaturowa – informacja geologiczna i procedury prawne*. Przegląd Geologiczny, vol. 63, nr 12/1, 2015, pp. 1388–1396.

[4] Śliwa T. (red.): *Zintegrowany system otworowych wymienników ciepła i kolektorów słonecznych*. Wydawnictwa AGH, Kraków 2012.

[5] Śliwa T.: *Badania podziemnego magazynowania ciepła za pomocą kolektorów słonecznych i wymienników otworowych*. Wydawnictwa AGH, Kraków 2012.

[6] Wołszyn J.: *Badania wpływu rozmieszczenia wymienników na efektywność podziemnych magazynów energii*. Akademia Górniczo-Hutnicza/AGH University of Krakow, Kraków 2014 [doctoral thesis].

[7] Śliwa T., Wolan M., Mazur C., Wójtowicz T.: *Adaptacja istniejących i zlikwidowanych odwiertów na głębokie otworowe wymienniki ciepła. Technologia wykonania końcowego wyposażenia otworu do pozyskiwania ciepła z górotworu*. VII Ogólnopolski Kongres Geotermalny/7th Polish Geothermal Congress: 28–30 IX 2021 [unpublished conference paper].

[8] Eskilson P.: *Thermal analysis of heat extraction boreholes*. University of Lund, Sweden, Lund 1987 [doctoral thesis].

Journal of Geotechnology and Energy | vol. 40 | no. 4 | 2023 | pp. 15–21

https://doi.org/10.7494/jge.2023.40.4.6146

REVIEW

Marek Leszek Solecki

AGH University of Krakow, Faculty of Drilling, Oil & Gas
ORCID: 0000-0001-8637-8300
e-mail: marek.solecki@agh.edu.pl

DEFORMATION BANDS – MIGRATION PATHWAYS OR BARRIERS FOR HYDROCARBONS IN SEDIMENTARY ROCKS – MINI REVIEW

Date of submission:
03.06.2023

Date of acceptance:
9.12.2023

Date of publication:
29.12.2023

https://journals.agh.edu.pl/jge

Abstract: A mini review of the topic of deformation bands is presented in the paper. The concept of deformation bands is defined and their impact on the flow of fluids in porous sedimentary rocks is determined. Deformation bands are mm-thick low-displacement deformation zones which have intensified cohesion and lower permeability compared with ordinary fractures. This term was introduced in 1968 in material science, ten years later it appeared in the geological context. This microstructures can occur as barriers or migration pathways for hydrocarbons. Their role depends mainly on microstructural features, and they are also considered in reservoir modeling. The occurrence of deformation bands in Poland is also outlined and discussed - they have been described in Western Outer Carpathians (Magura and Silesia nappes).

Keywords: deformation bands, hydrocarbons, permeability, migration, fluid flow

1. Introduction

Deformation bands are mm-thick low-displacement deformation zones that tend to have intensified cohesion and lower permeability compared with ordinary fractures [1]. They mostly occur in porous sandstones [2] but have also been observed in chalk [3] and carbonates [4, 5]. These structures should be considered when looking into cores from clastic reservoirs due to their potential role as barriers or pathways to fluid flow [6–25]. In this paper, the author discusses the term deformation band and the influence of this specific kind of microstructure on petroleum engineering.

2. Deformation bands – characteristics and classification

The term "deformation bands" was introduced in 1968 by [26] in material science; in the geological context, it was first applied in 1978 [27, 28]. Since then, some researchers have studied the occurrence of this microscructure in many regions of the world, e.g. United States of America, Norway, Italy [29–33]. They also occur in Poland, especially in the Carpathians [34–36].

Below are the key features of deformation bands within the context of sediment deformation and porous rock, as outlined in [1].

I. Deformation bands are predominantly found in clastic rocks, particularly in porous sandstones. The development and progression of these bands are connected to the rotation and translation of grains, necessitating a specific level of porosity. Insufficient porosity will favor the formation of tension fractures, stylolites, and slip or shear surfaces instead (refer to Fig. 1).
II. A deformation band is distinct from a slip surface.
III. Deformation bands typically manifest as individual bands, band zones, or faulted bands.
IV. Even in instances where these bands extend for hundreds of meters, single bands seldom exhibit offsets exceeding a few centimeters.

There are also some differences between deformation bands and ordinary fractures. At first, they are thicker and present smaller offsets than slip surfaces of comparable length. Also, deformation bands increase cohesion, whilst cohesion decreases across ordinary fractures. What is more, they also show a reduction in porosity and permeability, whereas tension fractures and slip surface exhibit an increase of these parameters. The differences between deformation bands and "classical" fractures may influence fluid flow and have an impact on hydrocarbon and groundwater reservoirs, where deformation bands are likely to occur.

In terms of kinematics, deformation bands can be categorized into three types: dilation bands, shear bands, and compaction bands (refer to Fig. 1). The majority of deformation bands documented in the literature are identified as shear bands which are often characterized by compaction, commonly referred to as compaction shear bands.

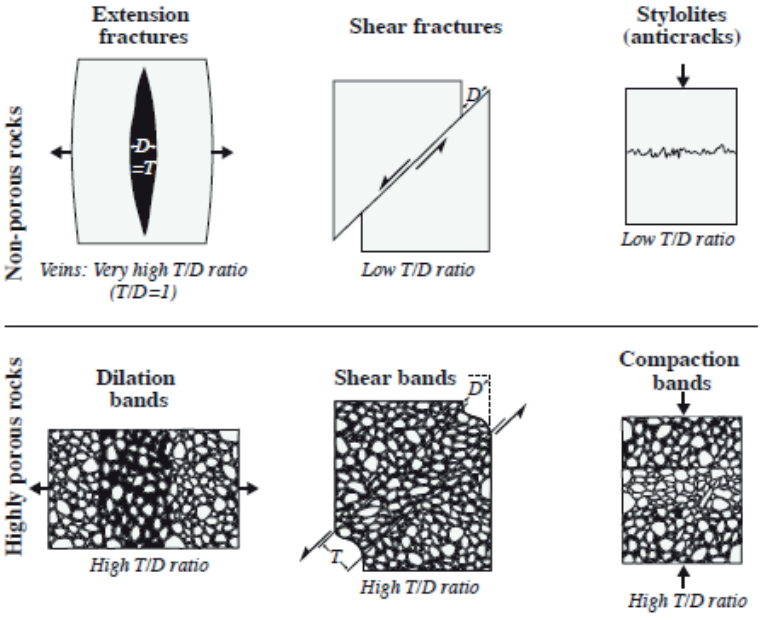

Fig. 1. Kinematic classification of deformation bands and their relationship to fractures in porous and non-porous rocks. *T*–thickness, *D*–displacement [2]

3. The influence of deformation bands on fluid flow

A visible reduction in permeability can be observed in most deformation bands, even by several orders of magnitude. However, the impact of these bands on fluid flow remains uncertain.

In the case of single-phase flow, such as oil moving through oil-saturated rock or water flowing in water-saturated rock, the key factors influencing Darcy flow are the permeability and thickness of deformation bands. Matthäi et al. [37] made numerical analyses in their paper of the impact of deformation bands on the reduction of permeability and fluid flow. The authors concluded that the influence of the bands on the reduction of these parameters is very small. Walsh et al. [38] considered that deformation bands only have significant effects on effective permeability when the ratio P^{DB}/P^{M} (deformation band permeability to matrix permeability) is less than 10^{-3}. Fossen and Bale [10] suggested the ratio as 10^{-4} and less. Nonetheless, Harper and Moftah [39] believed that zones of deformation bands were responsible for the reduction of productivity in some wells (the reduction of permeability in some fractures was even about 10%). Sample et al. [21] described the relationship between deformation bands and petroleum migration in the Monterey Formation. Sternlof et al. [40] in turn discussed the anisotropy of permeability – deformation bands parallel to the strike of a fault show higher values than those with a perpendicular strike, where fluids are more likely to encounter bands. The occurrence of deformation bands contributes to changes in the reservoir parameters of rocks; hence they are taken into account in reservoir modeling [41]. The influence of deformation bands on the flow of fluids through rock is illustrated in Figures 2 and 3.

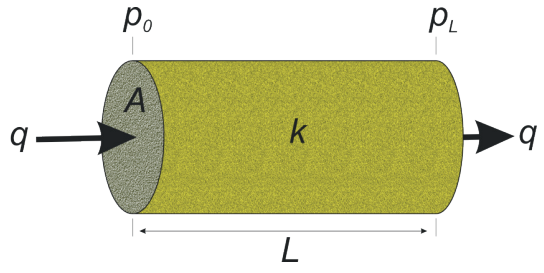

Fig. 2. Linear flow through a porous and homogeneous rock medium (sandstone) with permeability (k) (after [10])

Figure 2 depicts a linear flow system characterized by a consistent cross-sectional area (A) and a finite length (L). The medium possesses uniform permeability (k) and is saturated with an incompressible fluid of constant viscosity (m). Due to the incompressibility of the fluid, the flow rate (q) remains constant at all points within the system.

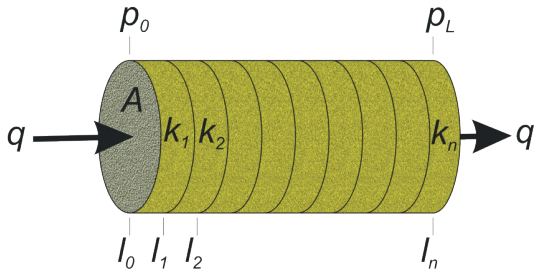

Fig. 3. Linear flow through a porous and heterogeneous rock medium (sandstone) composed of segments (deformation bands and surrounding rock) with distinct permeabilities (k_n) (after [10])

At Figure 3 a linear flow system comprising uniform segments arranged sequentially is illustrated. Each segment is characterized by a permeability that may vary from others, and the points where permeability changes occur are identified as (l_0, l_1, l_2, ..., l_n). The average permeability, denoted as (k_A), for a series of linear segments with distinct permeabilities is determined by dividing the length of each homogeneous segment by its permeability and summing these values for all segments. Subsequently, this sum is divided by the total length of the system (L).

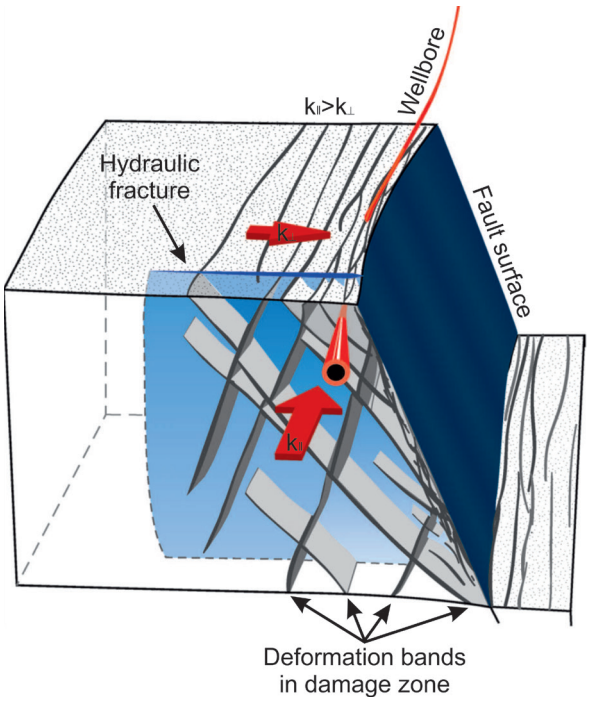

Fig. 4. A scheme showing the typical collocation of deformation bands in the destruction zone around the fault (after [10])

Figure 4 shows the collocation of deformation bands in the immediate vicinity of the damage zone surrounding the fault. The permeability measured parallel to the fault, denoted as ($k\parallel$), is higher than the permeability measured perpendicular to the fault, denoted as ($k\perp$), owing to the orientation of the deformation bands in relation to the fault.

4. The occurrence of deformation bands in Poland

To date, several places where deformation bands occur in Poland have been described. First, Aleksandrowski [42] described deformation bands in the Magura nappe near the Babia Góra Mountain region. Świerczewska and Tokarski [34, 43] and Tokarski et al. [44] described deformation bands in the Eocene strata of the Magura nappe in the Western Outer Carpathians near Tylmanowa and Gruszowiec. Nescieruk et al. [45] described structures called "step lineation" after [42] in the Krakowiec clays of the Sarmatian strata of the Carpathian Foredeep in the Sieniawa area. The occurrence of deformation bands in the Otryt facies of the Krosno sandstones of the Silesian nappe (Eastern Outer Carpathians) was reported by [35], as well as in the High Bieszczady part of the same tectonic unit (Figs. 5 and 6), in the valleys of Wołosaty, Dwernik and Solinka streams and in Połonina Wetlińska, Połonina Caryńska and Tarnica ranges [36, 46–50]. The Krosno sandstones constitute a regional layer of hydrocarbon reservoir rocks here.

Fig. 5. Krosno sandstone with deformation bands – outcrop near Dwernik village, deformation bands visible as "steps" on the rock

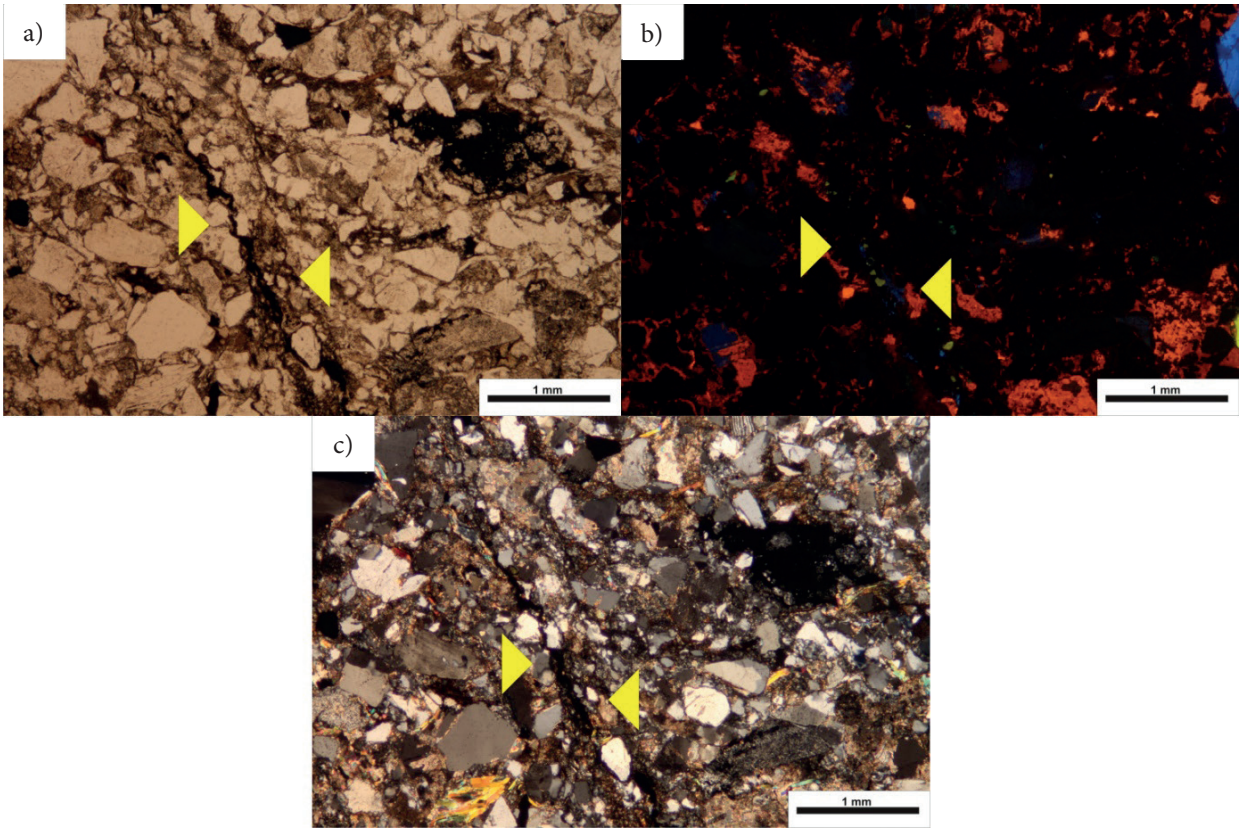

Fig. 6. Microphotographs showing the deformation bands (yellow arrows) in Krosno sandstone in a polarizing microscope: a) – parallel nicols; b) – cathodoluminescence (orange – calcite, blue – feldspar); c) – crossed nicols

5. Conclusions

Deformation bands are microstructures commonly found in sedimentary rocks (mainly sandstones, but also chalk and carbonates). They may act as barriers or privileged migration routes for fluids (e.g. hydrocarbons, water) in rocks. However, to significantly influence the petrophysical parameters of the rock, the ratio of their permeability to the permeability of the host rock should be at least 1:1000. This does not mean that deformation bands have no effect on the flow of fluids in rocks. Instead, their role mainly depends on microstructural features, and they are also considered in reservoir modeling.

Funding: This research was funded by the AGH University of Krakow subsidy No. 16.16.190.779 (Faculty of Drilling, Oil and Gas, Department of Petroleum Engineering).

References

[1] Fossen H., Schultz R.A., Shipton Z. K., Mair K.: *Deformation bands in sandstone: A review*. Journal of the Geological Society, vol. 164, 2007, pp. 755–769. https://doi.org/10.1144/0016-76492006-036
[2] Fossen H.: *Structural Geology*. Cambridge University Press, Cambridge, United Kingdom, 2016.
[3] Wennberg P.O., Casini G., Jahanpanah A., Lapponi F., Ineson J., Graham Wall B., Gillespie P.: *Deformation bands in chalk, examples from the Shetland Group of the Oseberg Field, North Sea, Norway*. Journal of Structural Geology, vol. 56, 2013, pp. 103–117. https://doi.org/10.1016/j.jsg.2013.09.005
[4] Cilona A., Baud P., Tondi E., Agosta F., Vinciguerra S., Rustichelli A., Spiers C.J.: *Deformation bands in porous carbonate grainstones: Field and laboratory observations*. Journal of Structural Geology, vol. 45, 2012, pp. 137–157. https://doi.org/10.1016/j.jsg.2012.04.012
[5] Rotevatn A., Thorsheim E., Bastesen E., Fossmark H.S.S., Torabi A., Sælen G.: *Sequential growth of deformation bands in carbonate grainstones in the hanging wall of an active growth fault: Implications for deformation mechanisms in different tectonic regimes*. Journal of Structural Geology, vol. 90, 2016, pp. 27–47. https://doi.org/10.1016/j.jsg.2016.07.003
[6] Antonellini M., Aydin A.: *Effect of faulting on fluid flow in porous sandstones: Geometry and spatial distribution*. AAPG Bulletin, vol. 79, 1995, pp. 642–671. https://doi.org/10.1306/8D2B1B60-171E-11D7-8645000102C1865D
[7] Antonellini M., Aydin A.: *Effect of faulting on fluid flow in porous sandstones: petrophysical properties*. AAPG Bulletin, vol. 78, 1994, pp. 355–377. https://doi.org/10.1306/BDFF90AA-1718-11D7-8645000102C1865D
[8] Antonellini M., Aydin A., Orr L.: *Outcrop-Aided Characterization of a Faulted Hydrocarbon Reservoir: Arroyo Grande Oil Field, California, USA*. In: Haneberg W.C., Mozley P.S., Moore C.J., Goodwin L.B. (eds), *Faults and Subsurface Fluid Flow in the Shallow Crust*. Geophysical Monograph Series, vol. 113, American Geophysical Union, Washington 1999, pp. 7–26. https://doi.org/10.1029/GM113p0007
[9] Beach A., Brown J.L., Welbon A.I., Mccallum J.E., Brockbank P., Knott S.: *Characteristics of fault zones in sandstones from NW England: application to fault transmissibility*. In: Meadows N.S., Trueblood S.P., Hardman M., Cowan G. (eds), *Petroleum Geology of the Irish Sea and Adjacent Areas*. Geological Society, Special Publications, vol. 124, The Geological Society, London 1997, pp. 315–324. https://doi.org/10.1144/GSL.SP.1997.124.01.19
[10] Fossen H., Bale A.: *Deformation bands and their influence on fluid flow*. AAPG Bulletin, vol. 91, no. 12, 2007, pp. 1685–1700. https://doi.org/10.1306/07300706146
[11] Gabrielsen R.H., Koestler A.G.: *Description and structural implications of fractures in late Jurassic sandstones of the Troll Field, northern North Sea*. Norsk Geologisk Tidsskrift, vol. 67, 1987, pp. 371–381.
[12] Gibson R.G.: *Physical character and fluid-flow properties of sandstone derived fault zones*. In: Coward M.P., Johnson H., Daltaban T.S. (eds), *Structural Geology in Reservoir Characterization*. Geological Society, Special Publications, vol. 127, The Geological Society, London 1998, pp. 83–97.
[13] Hesthammer J., Fossen H.: *Uncertainties associated with fault sealing analysis*. Petroleum Geoscience, vol. 6, 2000, pp. 37–45. https://doi.org/10.1144/petgeo.6.1.37
[14] Heynekamp M.R., Goodwin L.B., Mozley P.S, Haneberg W.C.: *Controls on fault zone architecture in poorly lithified sediments, Rio Grande Rift, New Mexico: Implications for fault zone permeability and fluid flow*. In: Haneberg W.C., Mozley P.S., Moore C.J., Goodwin L.B. (eds), *Faults and Subsurface Fluid Flow in the Shallow Crust*. Geophysical Monograph Series, vol. 113, American Geophysical Union, vol. 113, Washington 1999, pp. 27–49. https://doi.org/10.1029/GM113p0027.
[15] Jamison W.R., Stearns D.W.: *Tectonic deformation of Wingate Sandstone, Colorado National Monument*. AAPG Bulletin, vol. 66, 1982, pp. 2584–2608. https://doi.org/10.1306/03B5AC7D-16D1-11D7-8645000102C1865D

[16] Knipe R.J., Fisher Q.J., Clennell M.R. et al.: *Fault seal analysis: successful methodologies, application and future directions*. In: Møller Pedersen P., Koestler A.G. (eds), *Hydrocarbon Seals: Importance for Exploration and Production*. Norwegian Petroleum Society Special Publication, vol. 7, Elsevier, Amsterdam 1997, pp. 15–40. https://doi.org/10.1016/S0928-8937(97)80004-5.
[17] Lothe A.E., Gabrielsen R.H., Bjørnevoll Hagen N., Larsen B.T.: *An experimental study of the texture of deformation bands: effects on the porosity and permeability of sandstones*. Petroleum Geoscience, vol. 8, 2002, pp. 195–207. https://doi.org/10.1144/petgeo.8.3.195.
[18] Parnell J., Watt G.R., Middleton D., Kelly J., Baron M.: *Deformation band control on hydrocarbon migration*. Journal of Sedimentary Research, vol. 74, no. 4, 2004, pp. 552–560. https://doi.org/10.1306/121703740552.
[19] Pittman E.D.: *Effect of Fault-Related Granulation on Porosity and Permeability of Quartz Sandstones, Simpson Group (Ordovician), Oklahoma*. AAPG Bulletin, vol. 65, no. 11, 1981, pp. 238–2387. https://doi.org/10.1306/03B5999F-16D1-11D7-8645000102C1865D.
[20] Rotevatn A., Sandve T.H., Keilegavlen E., Kolyukhin D., Fossen H.: *Deformation bands and their impact on fluid flow in sandstone reservoirs: the role of natural thickness variations*. Geofluids, vol. 13, iss. 3, 2013, pp. 359–371. https://doi.org/10.1111/gfl.12030.
[21] Sample J.C., Woods S., Bender E., Loveall M.: *Relationship between deformation bands and petroleum migration in an exhumed reservoir rock, Los Angeles Basin, California, USA*. Geofluids, vol. 6, iss. 2, 2006, pp. 105–112. https://doi.org/10.1111/j.1468-8123.2005.00131.x.
[22] Shipton Z.K., Evans J.P., Robeson K., Forster C.B., Snelgrove S.: *Structural heterogeneity and permeability in faulted eolian sandstone: implications for subsurface modelling of faults*. AAPG Bulletin, vol. 86, no. 5, 2002, pp. 863–883. https://doi.org/10.1306/61EEDBC0-173E-11D7-8645000102C1865D.
[23] Shipton Z.K., Evans J.P., Thompson L.B.: *The geometry and thickness of deformation-band fault core and its influence on sealing characteristics of deformation-band fault zones*. In: Sorkhabi R., Tusuji Y. (eds), *Faults, Fluid Flow, And Petroleum Traps*. AAPG Memoir, vol. 85, American Association of Petroleum Geologists, Tulsa, Oklahoma 2005, pp. 181–195.
[24] Taylor W.L., Pollard D.D.: *Estimation of in situ permeability of deformation bands in porous sandstone, Valley of Fire, Nevada*. Water Resources Research, vol. 36, no. 9, 2000, pp. 2595–2606. https://doi.org/10.1029/2000WR900120.
[25] Zhang H.: *Fluid flow through deformation band*. Master Theses, no. 7577, 2016. https://scholarsmine.mst.edu/masters_theses/7577.
[26] Brown N., Duckett R.A., Ward I.M.: *Deformation bands in polyethylene terephtalate*. Journal of Physics D: Applied Physics, vol. 1, no. 10, 1968, pp. 1369–1379. https://doi.org/10.1088/0022-3727/1/10/317.
[27] Aydin A.: *Small faults formed as deformation bands in sandstone*. Pure and Applied Geophysics, vol. 116, 1978, pp. 913–930. https://doi.org/10.1007/BF00876546.
[28] Aydin A., Johnson A.M.: *Development of faults as zones of deformation bands and as slip surfaces in sandstones*. Pure and Applied Geophysics, vol. 116, 1978, pp. 913–930. https://doi.org/10.1007/BF00876547.
[29] Antonellini M.A., Aydin A., Pollard D.D.: *Microstructure of deformation bands in porous sandstones at Arches National Park, Utah*. Journal of Structural Geology, vol. 16, iss. 7, 1994, pp. 941–959. https://doi.org/10.1016/0191-8141(94)90077-9.
[30] Ballas G., Fossen H., Soliva R.: *Factors controlling permeability of cataclastic deformation bands and faults in porous sandstone reservoirs*. Journal of Structural Geology, vol. 76, 2015, pp. 1–21. https://doi.org/10.1016/j.jsg.2015.03.013.
[31] Exner U., Kaiser J., Gier S.: *Deformation bands evolving from dilation to cementation bands in a hydrocarbon reservoir (Vienna Basin, Austria)*. Marine and Petroleum Geology, vol. 43, 2013, pp. 504–515. https://doi.org/10.1016/j.marpetgeo.2012.10.001.
[32] Del Sole L., Antonellini M., Soliva R., Ballas G., Balsamo F., Viola G.: *Structural control on fluid flow and shallow diagenesis: insights from calcite cementation along deformation bands in porous sandstones*. Solid Earth, vol. 11, 2020, pp. 2169–2195, https://doi.org/10.5194/se-11-2169-2020.
[33] Tondi E., Antonellini M., Aydin A., Marchegiani L., Cello G.: *The role of deformation bands, stylolites and sheared stylolites in fault development in carbonate grainstones of Majella Mountain, Italy*. Journal of Structural Geology, vol. 28, iss. 3, 2006, pp. 376–391. https://doi.org/10.1016/j.jsg.2005.12.001.
[34] Świerczewska A., Tokarski A.K.: *Deformation bands and the history of folding in the Magura nappe, Western Outer Carpathians (Poland)*. Tectonophysics, vol. 297, iss. 1–4, 1998, pp. 73–90. https://doi.org/10.1016/S0040-1951(98)00164-4.
[35] Haczewski G., Kukulak J., Bąk K.: *Budowa geologiczna i rzeźba Bieszczadzkiego Parku Narodowego*. Wydawnictwo Naukowe Akademii Pedagogicznej, Kraków 2007.

[36] Solecki M.: *Rola mikrostruktur tektonicznych w zapisie migracji węglowodorów w skałach płaszczowiny śląskiej w dolinie potoku Wołosatego (Bieszczady)*. Master thesis, KSE WGGiOŚ AGH Archive, Kraków 2012.
[37] Matthäi S.K., Aydin A., Pollard D.D., Roberts S.G.: *Numerical simulation of departures from radial drawdown in a faulted sandstone reservoir with joints and formation bands*. In: Jones G., Fisher Q.J., Knipe R.J. (eds), *Faulting, Fault Sealing and Fluid Flow in Hydrocarbon Reservoirs*. Geological Society, Special Publications, vol. 147, The Geological Society, London 1998, pp. 157–191. https://doi.org/10.1144/GSL.SP.1998.147.01.11.
[38] Walsh J.J., Watterson J., Health A.E., Childs C.: *Representation and scaling of faults in fluid flow models*. Petroleum Geoscience, vol. 4, 1998, pp. 241–251. https://doi.org/10.1144/petgeo.4.3.241.
[39] Harper T.R., Moftah I.: *Skin Effect and Completion Options in the Ras Budran Reservoir*. In: *Middle East Oil Technical Conference and Exhibition: March 11–14, 1985, Bahrain*, SPE-13708-MS, Society of Petroleum Engineers, 1985, pp. 211–226.
[40] Sternlof K.R., Chapin J.R, Pollard D.D., Durlofsky L.J.: *Permeability effects of deformation bands arrays in sandstone*. AAPG Bulletin, vol. 88, no. 9, 2004, pp. 1315–1329.
[41] Qu D., Tveranger J.: *Incorporation of deformation band fault damage zones in reservoir models*. AAPG Bulletin, vol. 100, no. 3, 2016, pp. 423–443. https://doi.org/10.1306/12111514166.
[42] Aleksandrowski P.: *Step-like tectonic lineation in the Magura flysch (Western Outer Carpathians)*. Annales Societatis Geologorum Poloniae, vol. 50, no. 3–4, 1980, pp. 329–339.
[43] Świerczewska A., Tokarski A.K.: *Deformation development of a flysch sandstone, Outer Carpathians (Poland): from water escape structures to brittle faults*. In: *Abstracts: 30th International Geological Congress, Beijing, China, 4–14 August 1996. Vol. 2*, 1996, p. 269.
[44] Tokarski A.K., Świerczewska A., Banaś M.: *Deformation bands and early folding in Lower Eocene flysch sandstone, Outer Carpathians, Poland*. In: Rossmanith H.-P. (ed.), *Mechanics of Jointed and Faulted Rock*. Balkema, Rotterdam 1995, pp. 323–327.
[45] Nescieruk P., Wójcik A., Malata T., Aleksandrowski P.: *Tektoniczne struktury deformacyjne w iłach krakowieckich sarmatu w Wylewie k. Sieniawy (zapadlisko przedkarpackie): świadectwo młodej przesuwczej aktywności podłoża miocenu*. Przegląd Geologiczny, vol. 55, no. 8, 2007, pp. 690–698.
[46] Strzelecki P.J., Solecki M.L.: *Wpływ mikrotekstury i procesu kwasowania skały na jej parametry zbiornikowe: studium przypadku piaskowców krośnieńskich z rejonu Dwernika, Bieszczady* [*The influence of rock microtexture and acidizing on reservoir properties: a case study of the Krosno Sandstones from Dwernik, Bieszczady Mts.*]. Przegląd Geologiczny, vol. 69, nr 7, 2021, pp. 454–457. https://doi.org/10.7306/2021.30.
[47] Strzelecki P.J., Świerczewska A.: *Wpływ więźby skały na mechanizm deformacji: studium przypadku wstęg deformacyjnych w piaskowcach otryckich (Bieszczady)* [*The impact of rock fabric on deformation: a case study of deformation bands in the Otryt sandstone (Bieszczady Mountains, SE Poland)*]. Przegląd Geologiczny, vol. 71, 2023, pp. 231–234. https://doi.org/10.7306/2023.20
[48] Strzelecki P., Świerczewska A.: *Pure compaction bands in the naturally deformed flysch sandstones of the Silesian Nappe (SE Poland): early markers of tectonic shortening*. EGU General Assembly, 2023, EGU23-14083, https://doi.org/10.5194/egusphere-egu23-14083
[49] Strzelecki P.J., Świerczewska A., Tokarski A.K.: *Structural Evolution of the Eastern Part of the Silesian Nappe Recorded in Deformation Bands, Polish Segment of the Outer Carpathians*. Geology, Geophysics & Environment, vol. 44, no. 1, 2018, p. 196.
[50] Strzelecki P.J., Świerczewska A., Tokarski A.K.: *Do Deformation Bands Record the Early Onset of Backthrusting?: Insights from the Inner Part of the Silesian Nappe (outer Western Carpathians, Poland)*. In: Hrdličková K., Daňková L. (eds), *CETEG 2019: 17th Meeting of the Central European Tectonic Groups: Rozdrojovice, 24–27 April, 2019: Abstract Volume*. Czech Geological Survey, Prague 2019, pp. 79–80.

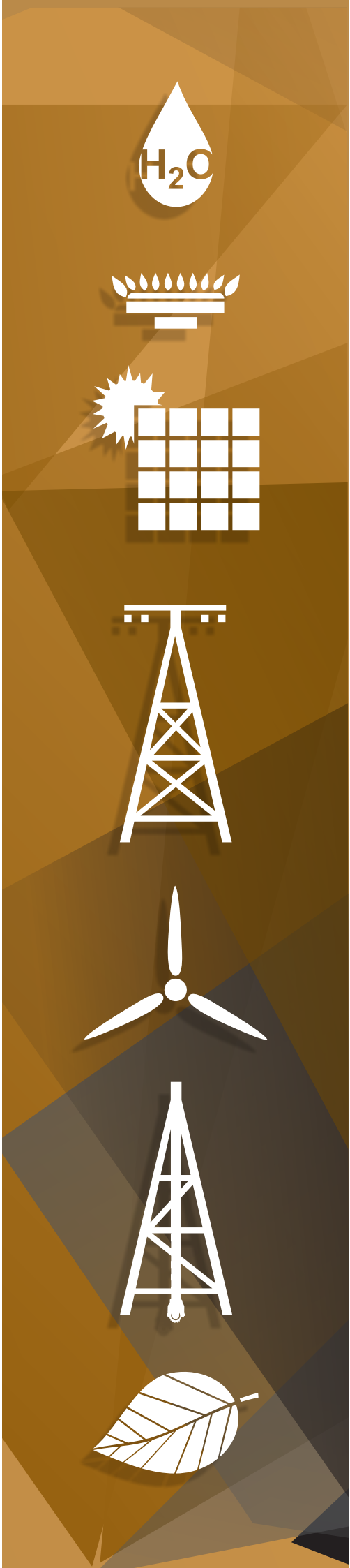
H2O